2014

Cu2ZnSnS4-Au heterostructures: Toward green photocatalytic materials active under visible light

Patrick Steven Dilsaver
Iowa State University

Cu_2ZnSnS_4-Au heterostructures: Toward green photocatalytic materials active under visible light

by

Patrick Steven Dilsaver

A thesis submitted to the graduate faculty

in partial fulfillment of the requirements for the degree of

MASTER OF SCIENCE

Major: Chemistry

Program of Study Committee:
Javier Vela, Major Professor
L. Keith Woo
Wenyu Huang

Iowa State University

Ames, Iowa

2014

TABLE OF CONTENTS

ACKNOWLEDGMENTS

I would first like to thank my advisor, Javier Vela, for his guidance and support the last few years. I learned a lot while working in his group and I will always be thankful for that, as well as the late night sesame chicken in Dallas. I would also like to thank Wenyu Huang and Keith Woo for serving on my committee and for their excellent teaching in the classroom and out.

I owe a lot to my parents, Steven and Linda Dilsaver, and would like to thank them for everything they have done for me over the years. A lot of parents tell their kids they can do whatever they want. Not many parents offer the kind of support and encouragement I have received throughout my time in college and grad school. I will always be appreciative of everything they have provided me with and the sacrifices they made.

My time in the Vela group would not have been so fun without the people I met and was forced to hang out with on a daily basis. In particular I would like to thank Malinda Reichert and Yijun Guo for always being my partners in crime when I wanted to get out of the office or go find a workout class. Thanks to Michelle for figuring out some of the harder tricks to working with CZTS so I didn't have to. Thanks to Chia-Cheng and Long for playing basketball, racquetball and teaching me some fun new Chinese phrases. I would also like to thank Sam Alvarado for his help and advice on my projects. Next thanks to Brad Schmidt, you've been a great friend and introduced me to a lot of great people while I've been here. You aren't in the Vela group, but not important enough for your own paragraph.

I would finally like to thank Jenna Malmquist, who was always there to listen and support me, and is important enough for her own paragraph. In addition to this she provided a

lot of help creating and designing some of the figures I use here and in presentations. Thank you Jenna, I couldn't have done it without you.

ABSTRACT

Solar energy is a potentially limitless source of clean power, but needs an effective means of conversion and storage to be feasible. Semiconductor-metal heterostructures have been studied as potential photocatalysts for use in solar-to-chemical energy conversion as a way of converting solar energy. This thesis examines pathways towards the synthesis of Cu_2ZnSnS_4-Au, a novel semiconductor-metal heterostructure. Cu_2ZnSnS_4 (CZTS) is attractive for use in this area because it has a narrow bandgap (1.5 eV) and is made of relatively earth-abundant and non-toxic elements.

There are four methods studied in this thesis for the fabrication of CZTS-Au, two use $AuCl_3$ as a precursor and two utilize pre-formed Au nanoparticles. Both precursors were studied under thermal and photochemical deposition conditions. The resulting products were characterized to determine the most effective pathway to fabricate these heterostructures. $AuCl_3$ under thermal deposition conditions proved to be the best pathway due to the well-defined monodisperse product.

We also studied whether Au metal islands could be effectively removed while leaving the CZTS nanocrystals intact. The results of this experiment were mixed. It does seem that smaller Au nanoparticles are removed, but larger amalgams remain attached to the CZTS nanorods and remain inseparable despite numerous efforts.

Finally, CZTS-Au was tested for photocatalytic activity using the model system of methylene blue reduction. CZTS-Au was found to convert methylene blue to leucomethylene blue at a much higher rate than bare CZTS. These results open up a new area of CZTS-metal

heterostructures for the purpose of finding greener photocatalysts for solar-to-chemical energy conversion.

CHAPTER 1

INTRODUCTION

General Introduction

This thesis describes progress toward the fabrication of non-toxic, earth abundant metal-semiconductor heterostructures for use in solar energy conversion. The proposed heterostructures consist of Cu_2ZnSnS_4 (CZTS) nanorods decorated with Au metal islands (Figure 1). The semiconductor nanorods are able to absorb light; generating electron-hole pairs (excitons). The Au metal islands promote charge separation and slow recombination of the electron-hole pairs. They can also serve as a platform for redox catalysis to take place. This work focuses first on the fabrication, control and characterization of these CZTS-Au heterostructures. The photocatalytic activity of these heterostructures is then explored with the reduction of methylene blue.

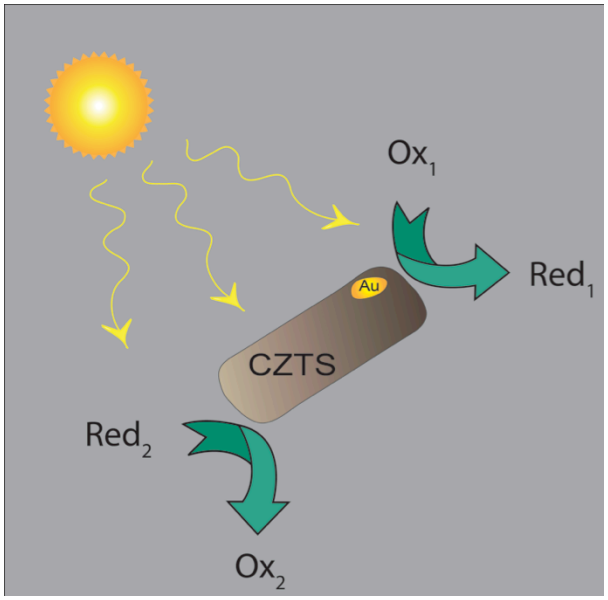

Figure 1: CZTS-Au photocatalyst design

Solar Energy Conversion

A reliable source of renewable, carbon-free or carbon-neutral energy is much needed. The concentration of CO_2 in the atmosphere has been rising since the beginning of the industrial age as a result of burning fossil fuels for energy. This has been linked to recent climate change and global warming.[1-4] The detrimental effects of global warming and rising CO_2 levels have on the ecosystem is also well documented.[5-8] These include the melting of polar ice caps, ocean acidification and an increase in extreme weather. It is clear that finding an energy source that does not result in additional CO_2 or other greenhouse emissions should be a priority.

A very promising source of cheap, abundant and carbon free energy is the Sun. The energy the Earth receives from the Sun in one hour is enough to meet the current energy needs of the entire planet for one year.[9, 10] This makes solar energy a practically limitless energy source if sunlight can be converted to either fuel or chemical energy (photocatalysis) or power (photovoltaics). Conversion of solar energy has already been proven feasible with the use of photocatalytic and photovoltaic (solar cell) devices. However, solar power is not currently cost-effective. Increasing the efficiency and reducing the cost of solar energy conversion devices is a very active and competitive area of research.[11, 12] Even if it were possible to convert sunlight with high-efficiency, there would still be significant problems with solar energy. One of the major issues with solar energy is its intermittent nature. During the night and when it is cloudy out, solar power output is dramatically reduced. People require energy at all times regardless of time or weather. A solution to this problem is to store the energy produced from sunlight for later use, either in the form of power (in batteries) or as fuel. This method for storing energy also needs to be cost-effective, and have the ability to

be scaled up. There are a few proposals for how to accomplish this, but all have problems. One such solution would be to simply store the power in batteries. Unfortunately, current battery technology does not make this cost-effective and can be an inefficient method of storing energy.[9] Lithium-ion batteries are too expensive to be used on such a wide-scale, and lead-acid batteries have relatively short lifetimes. Other methods of storing energy have been proposed such as compressed air, pumped hydro and flywheels, but all have issues with scaling and cost.[13]

A promising way of harnessing solar energy and storing it for later usage is to use this energy to make chemical bonds.[9, 14] This involves using solar energy to drive uphill (endergonic or endothermic) chemical reactions that create fuels which can be used as needed. One major benefit of this photocatalysis method is that the resulting fuel could be used in vehicles in addition to providing power to homes. Splitting water (H_2O) to produce hydrogen (H_2) and oxygen (O_2) is easily the most studied system for photocatalytic solar energy conversion.[15-18] This is an area of research that has been given much attention for good reason. Water splitting would provide an energy source, H_2, that combusts without carbon emissions and only results in water as a by-product. Water is also one of the most abundant resources we have on earth, so utilizing it seems to be a wise choice. Another interesting photocatalytic system is the reduction of CO_2 into more useful hydrocarbon fuels or feedstocks.[19, 20] This would be effectively carbon-neutral as one could take the CO_2 already found in the atmosphere and re-use it as fuel. One could also think about capturing CO_2 as it is produced at power plants for sequestration to combat climate change.

Both water splitting and CO_2 reduction are thermodynamically uphill processes. They will require energy to be put into the system in order to drive them forward. Photocatalysts

can utilize the energy from the sun to drive these uphill reactions forward. Semiconductor nanocrystals have garnered attention for use in photocatalysis.[21, 22]

Metal-semiconductor heterostructures as photocatalysts

Semiconductor nanocrystals are interesting candidates for solar energy conversion because they can absorb light to generate electron-hole (exciton) pairs that can be used in redox reactions such as water splitting (Figure 2). Light of sufficient energy (photons whose energy is equal to or higher than the band gap energy) is absorbed by the semiconductor and an electron is promoted from the valence band to the conduction band. This also generates a hole in the valence band. The electrons in the conduction band can then reduce a substrate if they have a sufficient redox potential. Likewise the holes in the valence band can oxidize a substrate.

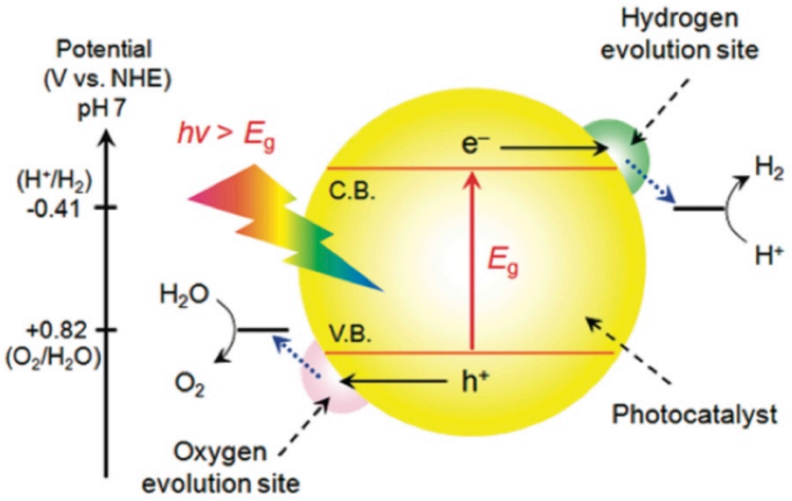

Figure 2: Diagram depicting how a semiconductor can be used as a photocatalyst. Reprinted with permission from *J. Phys. Chem. Lett.* **2010**, *1*, 2655-2661. Copyright 2010 © American Chemical Society.[15]

Of particular interest are semiconductor nanorods, which have the ability to generate multiple excitons upon irradiation and have a high surface to volume ratio.[23, 24] These properties are desirable for photocatalysis and for this purpose nanorods are the preferred morphology when designing semiconductor photocatalysts.

There has been much interest recently in metal-semiconductor heterostructures for use in solar energy conversion.[25-27] Depositing metal islands on the surface of semiconductors is known to enhance photocatalytic activity.[28] It is thought that this enhancement occurs because metal islands can slow the recombination rate. Electron-hole recombination competes directly with any photocatalytic process and is therefore highly undesired. In addition to this, noble metal islands have been shown to prevent degradation of the semiconductor from photoetching.[29] Metal islands can also act as a place for reaction with a substrate. These factors led us to believe that semiconductor-metal heterostructures, particularly nanorod heterostructures, were an interesting candidate for solar energy conversion and worthy of further study.

When looking for semiconductor-metal systems to use in photocatalysis, there are several key issues to address. It is important that the semiconductor be able to absorb a large portion of the visible spectrum, so as to more efficiently utilize the solar energy we receive on earth. Another issue is the relative abundance of the elements used in the materials. If these systems are to be utilized on a large-scale and be cost-effective, they need to exploit elements that are found in many places and are inexpensive. Yet another consideration is the toxicity of the material. It would be ideal if the material were relatively non-toxic so as to minimize any environmental effects. These materials would likely be used in close proximity to cities and homes, so any leaching or waste from the material could affect a large number

of people. These considerations led us to Cu_2ZnSnS_4 as an interesting semiconductor for use in photocatalysis.

Cu_2ZnSnS_4 as an Earth-abundant, non-toxic photocatalyst

Cu_2ZnSnS_4 (CZTS) has a bandgap of around 1.5 eV, corresponding to light with a wavelength of around 826 nm. This is comparable to CdSe (1.7 eV), which has been studied extensively as a photocatalyst. This smaller bandgap means that CZTS can absorb most of the solar spectrum. CZTS is also made of relatively earth-abundant materials, in comparison with a material such as CdSe.[30] It is also considered less toxic than CdSe. All of these factors led us to believe that CZTS was an interesting candidate for use in photocatalysis.

After choosing a semiconductor material to work with, we needed a method to prepare a CZTS-M heterostructure. There are multiple pathways reported in the literature for preparing these heterostructures. Thermal and photochemical methods have been used to deposit metals onto CdS and CdSe nanorods.[31, 32] These syntheses involve the use of metal salts as precursors for the noble metal nanoparticles formed on the semiconductor. Another approach to fabricating these heterostructures is to use pre-formed metal nanoparticles and deposit these onto the surface of the semiconductor.[33] Since CZTS is a relatively new material, there currently is no research to our knowledge of how best to deposit metal islands. We therefore decided it would be prudent to investigate all of the pathways mentioned above, and determine the best route to the desired CZTS-M heterostructure.

CdSe-Au has been used previously in photocatalysis.[34] Because of this, we chose Au as the metal to deposit on the surface of CZTS nanorods. Since CZTS and CdSe have similar bandgaps and band energy level offsets this would offer a good comparison between the two materials. Although Au is by no means an abundant element it will still be a good model

system to demonstrate photocatalytic activity with. This thesis therefore presents work investigating both Au salt precursors and pre-formed Au nanoparticles to deposit Au nanoparticles on CZTS nanorods under thermal and photochemical conditions. This thesis also presents research on removing the metal islands from the CZTS nanorods. The heterostructures were then probed for photocatalytic activity by using methylene blue reduction as a model system.

References

[1] Caldeira, K.; Jain, A.; Hoffert, M. Climate Sensitivity Uncertainty and the Need for Energy Without CO_2 Emission. *Science* **2003**, *299*, 2052-2054.

[2] Wigley, T. Analytical Solution for the Effect of Increasing CO_2 on Global Mean Temperature. *Nature* **1985**, *315*, 649-652.

[3] Frölicher, T.; Winton, M.; Sarmiento, J. Continued Global Warming After CO_2 Emissions Stoppage. *Nature Climate Change* **2014**, *4*, 40-44.

[4] Etheride, D.M.; Steeple, L.P.; Langenfelds, R.L.; Francey, R.J. Natural and Antropogenic Changes in Atmospheric CO_2 Over the Last 1000 Years From Air in Antartic Ice and Firn. *J. Geophys. Res.* **1996**, *101*, 4114-4128.

[5] Easterling, D.; Meehl, G.; Parmesan, C.; Changnon, S.; Karl, T.; Mearns, L. Climate Extremes: Observations, Modeling, and Impacts. *Science* **2000**, *289*, 2068-2074.

[6] Norby, R.; Luo, Y. Evaluating Ecosystem Responses to Rising Atmospheric CO_2 and Global Warming in a Multi-Factor World. *New Phytologist* **2004**, *162*, 281-293.

[7] Doney, S.; Fabry, V.; Feely, R.; Kleypas, J. Ocean Acidification: The Other CO_2 Problem. *Annu. Rev. Mar. Sci.* **2009**, *1*, 169-192.

[8] Spencer, J.; Rodolfo-Metalpa, R.; Martin, S.; Ransome, E.; Fine, M.; Turner, S.; Rowley, S.; Tedesco, D.; Buia, M-C. Volcanic Carbon Dioxide Vents Show Ecosystem Effects of Ocean Acidification. *Nature* **2008**, *454*, 96-99.

[9] Crabtree, G.; Lewis, N. Solar Energy Conversion. *Physics Today* **2007**, *60*, 37-42.

[10] Lewis, N. Toward Cost-Effective Solar Energy Use. *Science* **2007**, *315*, 798-801.

[11] Parida, B.; Iniyan, S.; Goic, R. A Review of Solar Photovoltaic Technologies. *Renew. Sust. Energ. Rev.* **2011**, *15*, 1652-1636.

[12] Green, M.; Emery, K.; Hishikawa, Y.; Warta, W.; Dunlop, E. Solar Cell Efficiency Tables. *Prog. Photovolt: Res. Appl.* **2012**, *20*, 12-20.

[13] Cook, T.; Dogutan, D.; Reece, S.; Surendranath, Y.; Teets, T.; Nocera, D. Solar Energy Supply and Storage for the Legacy and Nonlegacy Worlds. *Chem. Rev.* **2010**, *110*, 6474-6502.

[14] Kamat, P. Meeting the Clean Energy Demand: Nanostructure Architectures for Solar Energy Conversion. *J. Phys. Chem. C* **2007**, *111*, 2834-2860.

[15] Maeda, K.; Domen, K. Photocatalytic Water Splitting: Recent Progress and Future Challenges. *J. Phys. Chem. Lett.* **2010**, *1*, 2655-2661.

[16] Miseki, Y.; Kudo, A. Heterogeneous Photocatalyst Materials for Water Splitting. *Chem. Soc. Rev.* **2009**, *38*, 253-278.

[17] Ni, M.; Leung, M.; Leung, D.; Sumathy, K. A Review and Recent Developments in Photocatalytic Water-Splitting Using TiO_2 for Hydrogen Production. *Renew. Sust. Ener. Rev.* **2007**, *11*, 401-425.

[18] Walter, M.; Warren, E.; McKone, J.; Boettcher, S.; Mi, Q.; Santori, E.; Lewis, N. Solar Water Splitting Cells. *Chem. Rev.* **2010**, *110*, 6446-6473.

[19] Hoffmann, M.; Moss, J.; Baum, M. Artificial Photosynthesis: Semiconductor Photocatalytic Fixation of CO_2 to Afford Higher Organic Compounds. *Dalton Trans.* **2011**, *40*, 5151-5158.

[20] Indrakanti, V.; Kubicki, J.; Schobert, H. Photoinduced Activation of CO2 on Ti-Based Heterogeneous Catalysts: Current State, Chemical Physics-Based Insights and Outlook. *Energy Environ. Sci.* **2009**, *2*, 745-758.

[21] Kisch, H. Semiconductor Photocatalysis-Mechanistic and Synthetic Aspects. *Angew. Chem. Int. Ed.* **2013**, *52*, 812-847.

[22] Maldotti, A.; Molinari, A.; Amadelli, R. Photocatalysis with Organized Systems for the Oxofunctionalization of Hydrocarbons by O_2. *Chem. Rev.* **2002**, *102*, 3811-3836.

[23] Klimov, V. Mechanisms for Photogeneration and Recombination of Multiexcitons in Semiconductor Nanocrystals: Implications for Lasing and Solar Energy Conversion. *J. Phys. Chem. B.* **2006**, *110*, 16827-16845.

[24] Nozik, A. Multiple Exciton Generation in Semiconductor Quantum Dots. *Chem. Phys. Lett.* **2008**, *457*, 3-11.

[25] Costi, R.; Saunders, A. Banin, U. Colloidal Hybrid Nanostructures: A New Type of Functional Materials. *Angew. Chem. Int. Ed.* **2010**, *49,* 4878-4897.

[26] Banin, U.; Ben-Shahar, Y.; Vinokurov, K. Hybrid Semiconductor-Metal Nanoparticles: From Architecture to Function. *Chem. Mater.* **2014**, *26*, 97-110.

[27] Linic, S.; Christopher, P.; Ingram, D. Plasmonic Nanostructures for Efficient Conversion of Solar to Chemical Energy. *Nat. Mater.* **2011**, *10*, 911-921.

[28] Vaneski, A.; Susha, A.; Rodriquez-Fernandez, J.; Berr, M.; Jackel, F.; Rogach, A. Hybrid Colloidal Heterostructures of Anisotropic Semiconductor Nanocrystals Decorated with Noble Metals: Synthesis and Function. *Adv. Funct. Mater.* **2011**, *21*, 1547-1556.

[29] Ruberu, T.A.; Nelson, N.; Slowing, I.; Vela, J. Selective Alcohol Dehydrogenation and Hydrogenolysis with Semiconductor-Metal Photocatalysts: Toward Solar-to-Chemical Energy Conversion of Biomass-Relevant Substrates. *J. Phys. Chem. Lett.* **2012**, *3*, 2798-2802.

[30] Wedepohl, K. The Composition of the Continental Crust. *Geochimica et Cosmochimica Acta* **1995**, *59*, 1217-1232.

[31] Dukovic, G.; Merkle, M.; Nelson, J.; Hughes, S.; Alivisatos, A.P. Photodeposition of Pt on Colloidal CdS and CdSe/CdS Semiconductor Nanostructures. *Adv. Mater.* **2008**, *20*, 4306-4311

[32] Saunders, A.; Popov, I.; Banin, U. Synthesis of Hybrid CdS-Au Colloidal Nanostructures. *J. Phys. Chem. B.* **2006**, *110*, 25421-25429.

[33] Alemseghed, M.; Ruberu, T.P.; Vela, J. Controlled Fabrication of Colloidal Semiconductor-Metal Hybrid Heterostructures: Site Selective Metal Photo Deposition. *Chem. Mater.* **2011**, *23*, 3571-3579.

[34] Costi, R.; Saunders, A.; Elmalem, E.; Salant, A.; Banin, U. Visible Light-Induced Charge Retention and Photocatalysis with Hybrid CdSe-Au Nanodumbbells. *Nano Lett*. **2008**, *8*, 637-641.

CHAPTER 2

Cu_2ZnSnS_4-Au HETEROSTRUCTURES: TOWARD GREENER CHALCOGENIDE-BASED PHOTOCATALYTS

A paper submitted to The Journal of Physical Chemistry C

Patrick S. Dilsaver, Malinda D. Reichert, Brittany L. Hallmark, Michelle J. Thompson, and Javier Vela*

Abstract

Chalcogenide-based semiconductor-metal heterostructures are interesting catalysts for solar-to-chemical energy conversion, but current compositions are impractical due to the relative toxicity and/or scarcity of their constituent elements. To address these concerns, Cu_2ZnSnS_4 (CZTS) emerged as an interesting alternative to other chalcogenide-based semiconductors, however the fabrication of CZTS-metal heterostructures remains unexplored. In this paper, we systematically explore four methods of synthesizing CZTS-Au heterostructures, specifically: Reaction of CZTS nanorods with either a soluble molecular gold precursor ($AuCl_3$) or preformed gold (Au) nanoparticles, each under thermal (heating in the dark) or photochemical reaction conditions (350 nm lamp illumination at room temperature). We find that using $AuCl_3$ under thermal deposition conditions results in the most well defined CZTS-Au heterostructures, containing >99% surface-bound 2.1±0.5 nm Au islands along the whole length of the nanorod. These CZTS-Au heterostructures are photocatalytically active, reducing the model compound methylene blue upon irradiation much more effectively than do bare CZTS nanorods. We also demonstrate the removal of Au from the CZTS-Au heterostructures by amalgamation. These results open up a new area of greener, CZTS-based photocatalysts for solar-to-chemical energy conversion.

Introduction

Semiconductor-metal hybrid heterostructures are ideal photocatalytic materials for the study of solar-to-chemical energy conversion.[1-13] Traditionally based on semiconductor oxides such as TiO_2[14-17], the field of semiconductor-metal hybrids saw a resurgence with the advent of colloidal II-VI, III-V and IV-VI semiconductor nanocrystals, particularly those made of cadmium and lead chalcogenides.[18-25] The semiconductor's photocatalytic activity, selectivity and stability greatly depend upon metal modification[26], and recent studies show that plasmonic effects even enable unprecedented switching and fine-tuning of overall photocatalytic behavior.[27-29] In an effort to replace cadmium, lead and arsenic-containing semiconductors, Cu_2ZnSnS_4 or "CZTS" recently emerged as one of the *photovoltaic* materials of choice for solar-to-*power* energy conversion.[30-32] Made of Earth abundant, widely distributed and relatively biocompatible elements, and with a direct band gap of 1.5 eV, Cu_2ZnSnS_4 is an affordable, greener and more sustainable alternative to cadmium and lead chalcogenides. However, the use of Cu_2ZnSnS_4 in *photocatalytic* semiconductor-metal heterostructures for solar-to-*chemical* energy conversion remains unexplored.[33-35]

Several reviews detail the fabrication and applications of low dimensional CZTS and CZTSe nanostructures.[36-41] Historically hindered by spontaneous phase segregation into binary and ternary impurities, colloidal CZTS nanocrystals are now accessible *via* solution-phase synthesis methods.[42-47] Anisotropic CZTS nanocrystals (nanorods, nanospindles, nanowires) are particularly attractive in order to achieve better charge carrier mobility across grain boundaries in photovoltaic cells, as well as more efficient suppression of electron-hole pair recombination in photocatalytic devices. Two recent reports looked at the interplay

between molecular precursor reactivity, precursor concentration, and the ability to make true quaternary anisotropic CZTS nanocrystals (CZTS nanorods).[48,49]

In this paper, we use wurtzite (hexagonal) phase CZTS nanorods as a template for the deposition of gold (Au) nanoparticles. More specifically, we learn to deposit Au on CZTS using both thermal and photochemical methods from either a molecular gold precursor or preformed Au nanoparticles. We then use the resulting semiconductor-metal CZTS-Au heterostructures for solar-to-chemical energy conversion using the photocatalytic reduction of methylene blue as a model reaction. Finally, we explore the removal or stripping of gold particles from CZTS-Au heterostructures via amalgamation upon treatment with mercury (Hg). The results of this work will serve as a springboard from which to build other greener, cost effective and more active, stable and selective semiconductor-metal hybrid heterostructures for solar-to-chemical energy conversion.

Results and Discussion

Multiple Metal Modification Methods. As noted in the Introduction above, metal heterostructures can be conveniently synthesized by either thermal or photochemical methods. Photochemical methods,[50-55] including whole flask lamp illumination methods[18] offer many advantages such as control over nanoparticle loading through fine-tuning of the illumination or "irradiation" time,[56] high selectivity for surface-bound *vs.* freestanding metal particles,[18] and selectivity for deposition along the length *vs.* the tip of anisotropic semiconductor particles (rods, wires).[57-59] Further, we noted during our work with CdE-M heterostructures (E = S or Se, M = Pt, Pd, Au)[18,26,27] that pre-existing metal nanoparticles, particularly those made of gold (Au), have a tendency to adhere to chalcogenide surfaces. We

thus hypothesized that we could deposit Au on CZTS not only from molecular gold precursors, but also possibly starting from preformed Au nanoparticles, in each case through either thermal or photochemical conditions.

Metal Deposition from a Molecular Precursor. We started using $AuCl_3$ as a soluble molecular precursor under *thermal* metal deposition conditions (60 °C in the dark, see Experimental). Transmission electron microscopy (TEM) showed this thermal procedure leads to well defined, monodisperse heterostructures with a homogeneous distribution of Au islands along the whole length of the CZTS nanorods (Figure 1a). The Au metal islands have an average size of 2.1±0.5 nm (Table 1). The great majority of Au particles (>99%) are surface-bound, meaning that they are attached to the surface of the CZTS nanorods. There are in average 9±2 Au metal islands per CZTS nanorod. Based on TEM measurements and within experimental error, the original length (28±3 nm) and diameter (8±1 nm) or aspect ratio (3.5±0.6) of the CZTS nanorods (Figure 2a) are unaffected upon thermal Au deposition from $AuCl_3$ (Table 1).

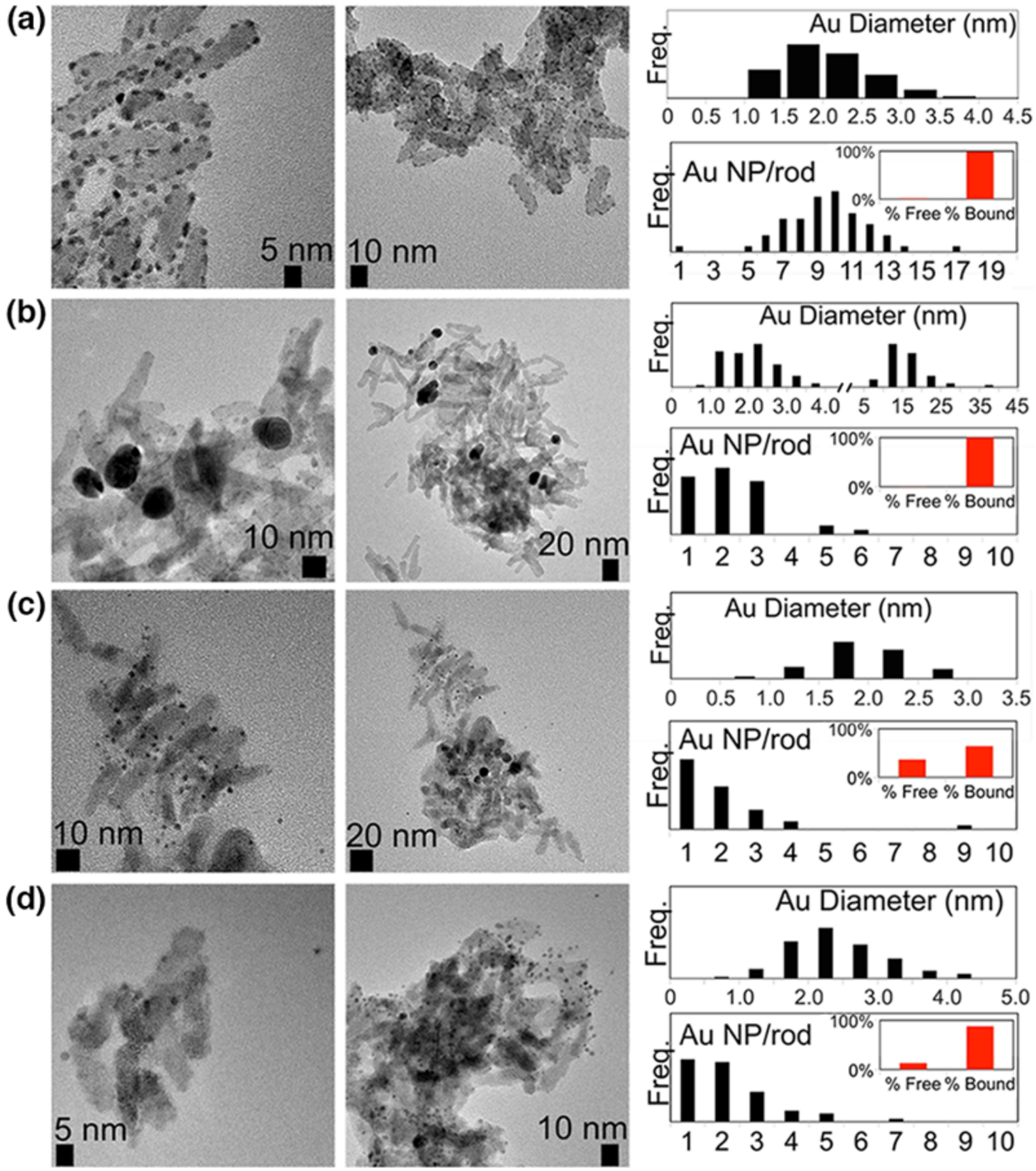

Figure 1. Representative TEM images and histograms of CZTS-Au heterostructures synthesized from $AuCl_3$ under (a) *thermal* conditions (60 °C, dark) and (b) under *photochemical* conditions (R.T., 350 nm), and from preformed Au nanoparticles under (c) *thermal* conditions (60 °C, dark) and (d) under *photochemical* conditions (R.T., 350 nm).

Table 1. Thermal and Photochemical Deposition of Au Nanoparticles on CZTS Nanorods.[a]

Au Precursor	Conditions[b]	Au Diameter[a]	%Au Bound[a]	#Au NP/rod[a]	CZTS Length[a]	CZTS Width[a]
$AuCl_3$	Dark, 60 °C	2.1±0.5 nm	> 99%	9±2	28±3 nm	8±1 nm
$AuCl_3$	350 nm, R.T.	8±6 nm	> 99%	2±1	27±5 nm	6±1 nm
Au NPs[c]	Dark, 60 °C	2.0±4 nm	64%	2±1	25±3 nm	8±1 nm
Au NPs[c]	350 nm, R.T.	2.4±0.6 nm	87%	2±1	26±4 nm	8±1 nm

[a]Post-deposition data for the resulting CZTS-Au heterostructures. [b]In all cases, the starting CZTS nanorods (before deposition) were 28±3 nm long and 8±1 nm wide (aspect ratio ≈ 3.5). [c]The starting Au nanoparticles (NPs) were 2.0±0.4 nm in diameter. (see Experimental for synthetic details)

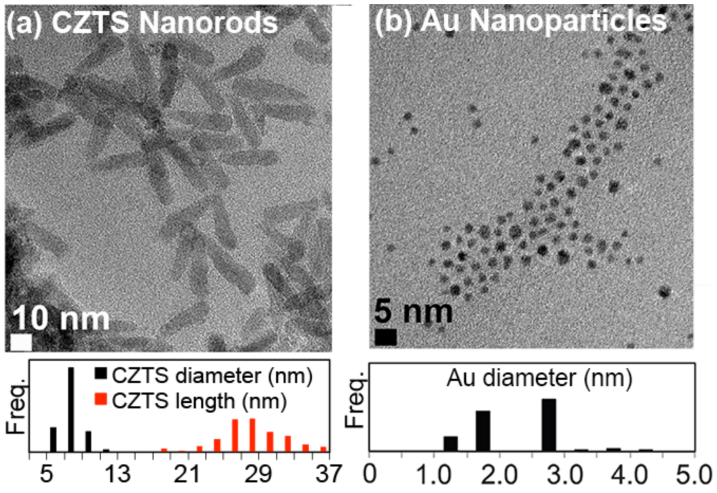

Figure 2. Representative TEM images and histograms for (a) CZTS nanorods (28±3 nm × 8±1 nm), and (b) independently synthesized preformed Au nanoparticles (2.0±0.4 nm).

The soluble $AuCl_3$ molecular precursor becomes much more reactive and deposition less controlled under *photochemical* deposition conditions (R.T. ≈ 21-24 °C at 350 nm, see Experimental). TEM shows the resulting heterostructures have a wider range of metal

particle sizes (Figure 1b). The Au nanoparticles have a bimodal size distribution with an average diameter of 8±6 nm (Table 1), although a majority of them (>99%) are also surface-bound. There is an average of only 2±1, larger Au metal islands per CZTS nanorod. TEM appears to indicate that etching of the CZTS occurs during photochemical Au deposition from $AuCl_3$, as the nanorod diameter changes from 8±1 nm before deposition to 6±1 nm after deposition. However, this difference is statistically insignificant within experimental error (Table 1).

Metal Deposition from Preformed Au Nanoparticles. We then attempted to use independently synthesized, preformed Au nanoparticles with a diameter of 2.0±0.4 nm for the synthesis of CZTS-Au heterostructures (Figure 2b). After reaction with CZTS under *thermal* deposition conditions (60 °C in the dark, see Experimental), TEM shows that the mean Au nanoparticle size (2.0±0.4 nm) remains similar to that of the preformed Au particles before reaction (Figure 1c). This is also comparable to the Au nanoparticle size obtained thermally from $AuCl_3$ above. However, in this case only 64% of Au particles are bound to the CZTS surface. Counting only surface-bound metal particles, there is an average of 2±1 Au islands per nanorod (Table 1). There is no evidence of changes in the length or diameter of the CZTS nanorods upon Au deposition by this method.

Under *photochemical* deposition conditions (R.T. ≈ 21-24 °C at 350 nm, see Experimental), the reaction of preformed Au nanoparticles with CZTS nanorods also results in a mixture of freestanding and surface bound gold. The mean Au nanoparticle size remains unchanged at 2.4±0.6 nm (Figure 1d). However, 87% of Au nanoparticles are now surface bound to the CZTS nanorods, an even higher percentage than that obtained thermally above. Counting only surface-bound metal particles, there is an average of 2±1 Au islands per

nanorod (Table 1). As in the previous example, there is no evidence of changes in the length or diameter of CZTS nanorods upon Au deposition by this method. However, the CZTS nanorods appear to be significantly aggregated after deposition.

Scheme 1 summarizes all of our deposition results. We note that using $AuCl_3$ as the gold precursor consistently leads to higher, near quantitative (100%) formation of surface bound Au nanoparticles, likely because of the lower activation energy required for heterogeneous (seeded) nucleation of Au on the CZTS surface *vs.* homogeneous nucleation of free Au in solution. Using preformed Au nanoparticles as precursors consistently leads to a smaller percentage of surface bound Au particles (64-87%). This percentage is nevertheless significant, and clearly demonstrates that nano gold avidly sticks to the soft, chalcogenide CZTS surface. The degree of attachment of Au particles is higher when the reaction is carried out photochemically (87%) than when it is carried out thermally (64%). It may well be that under illumination, enough negative charging occurs (for example, through electron trapping at defects sites) to make the CZTS surface even more polarizable and thus softer, increasing its affinity toward Au. In our previous work on photodeposition of Pt and Pd on CdS_xSe_{1-x},[18] we showed we could increase the number of surface-bound metal particles to near 100% by using a wavelength that selectively excites the semiconductor and not the metal precursor. This is difficult to achieve here because there is significant overlap between the absorption profiles of CZTS nanorods and the $AuCl_3$ and Au nanoparticle precursors (Figure 3a).

Scheme 1. Different pathways and outcomes of Au nanoparticle deposition on CZTS nanorods.

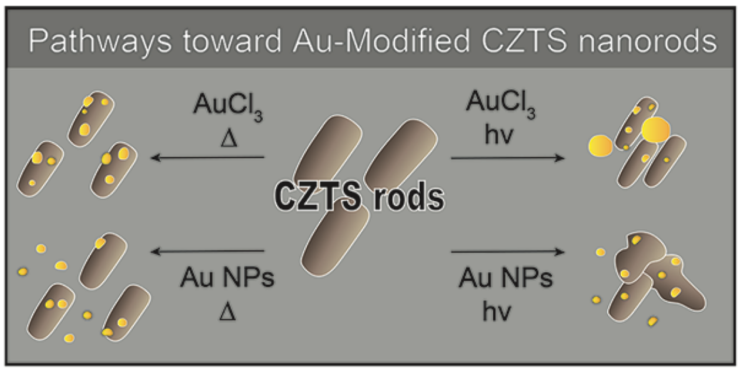

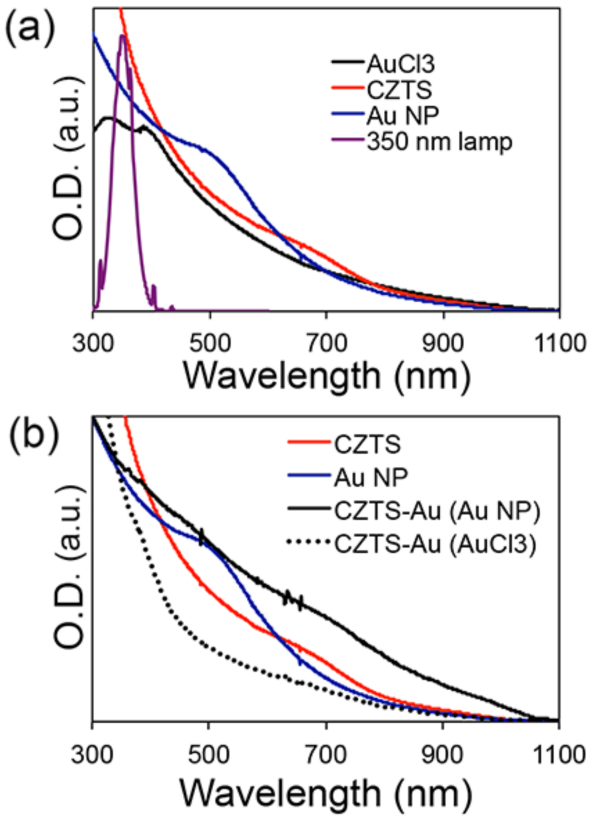

Figure 3. (a) Optical absorption spectra of the $AuCl_3$ molecular precursor, preformed Au nanoparticles and CZTS nanorods, and irradiation profile of 350 nm lamps. (b) Optical absorption spectra of preformed Au nanoparticles (Au NP), CZTS nanorods and CZTS-Au heterostructures obtained from different precursors.

Characterization of CZTS-Au Heterostructures. Figure 3b displays representative optical absorption spectra for the CZTS and Au nanoparticle precursors and the synthesized CZTS-Au heterostructures. The CZTS nanorods and all CZTS-Au heterostructures share the typical semiconductor absorption edge around 850-900 nm and a second bluer hump at 700 nm. The plasmonic resonance absorption feature at 500 nm observed in the preformed Au nanoparticles becomes broader, weakens and blue shifts to about 400 nm in the CZTS-Au heterostructures. Figure 4 shows powder X-ray diffraction (XRD) patterns of CZTS nanorods and CZTS-Au hybrids, along with standard reference patterns for both CZTS and Au. CZTS retains the previously reported wurtzite (hexagonal) structure and Au particles the common fcc metal structure.

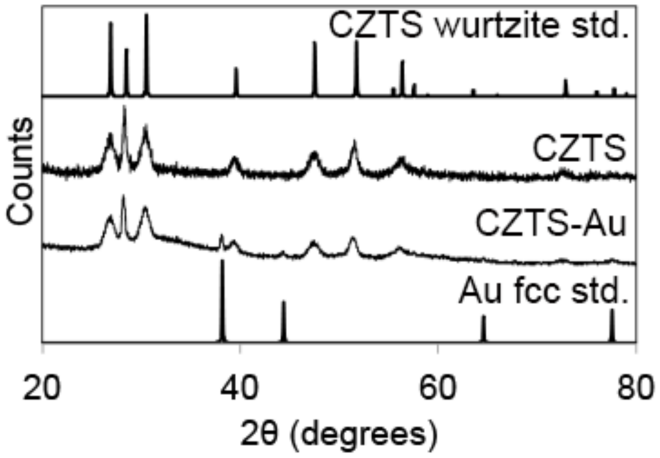

Figure 4. XRD diffraction patterns of CZTS before and after Au deposition. Standard bulk patterns for wurtzite (hexagonal) ZnS (in lieu of CZTS)[48] and metallic (fcc) Au are shown for comparison. The Au peaks are most intense when $AuCl_3$ is used as the gold precursor.

To further characterize the CZTS nanorods, Au nanoparticles and CZTS-Au heterostructures, we used X-ray photoelectron spectroscopy (XPS). Figure 5 shows the Cu 2p and Au 4f XPS spectral regions. Cu 2p shows the same binding energy before and after deposition. This is an indication that the oxidation state of Cu is unaffected by the deposition process. Because there is significant overlap in the binding energy values reported for Cu(I) and Cu(II), it is difficult to say with absolute certainty what the Cu oxidation state is in these materials from XPS data alone; however, we assume this is Cu(I) based on the known composition and crystal structure of CZTS observed by XRD. The CZTS nanorods do not show any Au 4f peaks before metal deposition, whereas the preformed Au nanoparticles and CZTS-Au heterostructures show characteristic Au 4f peaks (Figure 5). This serves as further confirmation that metallic, zerovalent Au was successfully deposited on the surface of the CZTS nanorods.

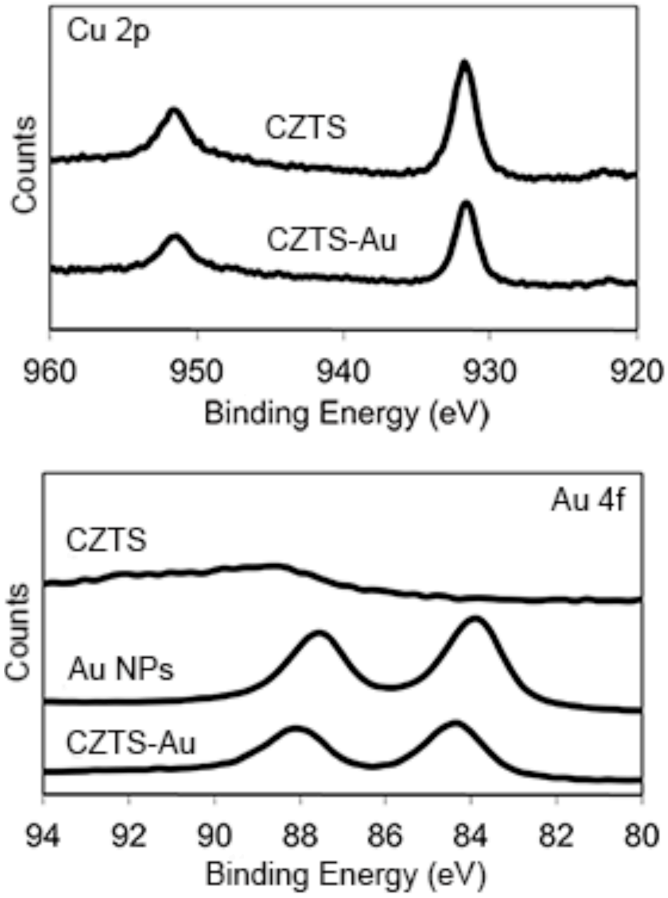

Figure 5. X-ray photoelectron spectroscopy (XPS) measurements of CZTS, Au and CZTS-Au nanostructures.

Photocatalytic Testing. The bulk band gap and valence and conduction energy levels of CZTS are similar to those of CdSe, a relatively better studied semiconductor with demonstrated photocatalytic activity (Figure 6). Previous reports showed that CdSe-Au hybrids can photocatalytically reduce methylene blue (M.B.) to the colorless product lecuomethylene blue (L.B.).[60-63] CZTS and CZTS-based heterostructures are therefore good catalyst candidates for this reaction, and we sought to use the reduction of methylene blue to test the photocatalytic activity of CZTS-Au hybrids. As a stoichiometric or "sacrificial" source of electrons, we chose to use an alcohol such as methanol. Reduction of methanol to

formaldehyde occurs at a lower potential than the reduction of M.B. to L.B., methanol cannot be expected to directly reduce M.B. (Figure 6). However, photogenerated electrons sitting in the conduction band of CZTS should have enough energy to reduce M.B., and photogenerated holes sitting in the valence band of CZTS should have enough energy to oxidize the sacrificial methanol donor, thus replenishing the electrons in the valence band of CZTS and regenerating the neutral ground state of the catalyst (Scheme 2).

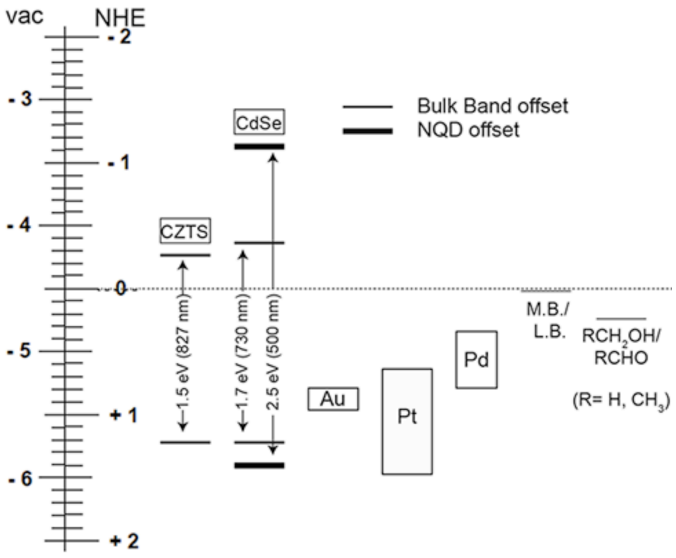

Figure 6. Valence and conduction bulk energy levels reported for CZTS and CdSe semiconductors, work functions for Au, Pt and Pd, and reduction potentials for methylene blue (M.B.) to leucomethylene blue (L.B.) and a primary alcohol to its aldehyde (such as methanol to formaldehyde). The "NQD" levels correspond to the maximum band gap widening reported for quantum confined CdSe. Note that Fermi level equilibration could significantly raise the energy the level of small Au nanoparticles, up to the conduction band of the CZTS semiconductor.[64]

Scheme 2. Photocatalytic reduction of methylene blue to leucomethylene blue over CZTS-Au heterostructures using an alcohol as sacrificial electron donor.

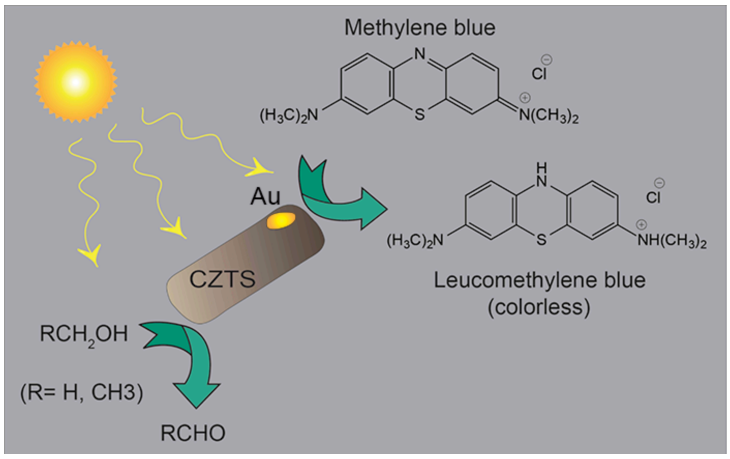

Photoinduced charge separation normally results in transfer of one carrier (for example, electrons) onto the metal islands of semiconductor-metal heterostructures. Figure 6 shows the energy levels of various metals commonly used in semiconductor-metal heterostructures, such as Au, Pt and Pd. From this diagram, it would appear that electrons sitting in any of these metals would never have enough energy to react with methylene blue. However, it is known and has been shown previously that the electrons transferred to small metal islands such as Au metal can significantly increase the electron density within the Au nanoparticles, shifting their Fermi level toward more negative potentials.[64] This transfer of electrons to the metal continues until the Fermi level equilibrates with the conduction band edge of the semiconductor, in this case CZTS.[64] This explains how electrons transferred to the Au metal from the CZTS semiconductor can have enough energy to reduce methylene blue (M.B.) to leucomethylene blue (L.B.).

Before running any photocatalytic tests and in order to select the best conditions for catalyzed methylene blue reduction, we carefully looked at the irradiance profiles of different

lamps as well as the optical absorption spectra of methylene blue and CZTS-Au heterostructures. As shown in Figure 7a, the light emitted by our 420 nm lamps does not have enough energy to directly photoexcite methylene blue, however it can easily photoexcite CZTS-based nanostructures such as CZTS-Au. Therefore, we decided to run our photocatalytic tests under 420 nm lamp illumination, as this prevents any uncatalyzed, direct reduction or other unwanted side-reactions of methylene blue.

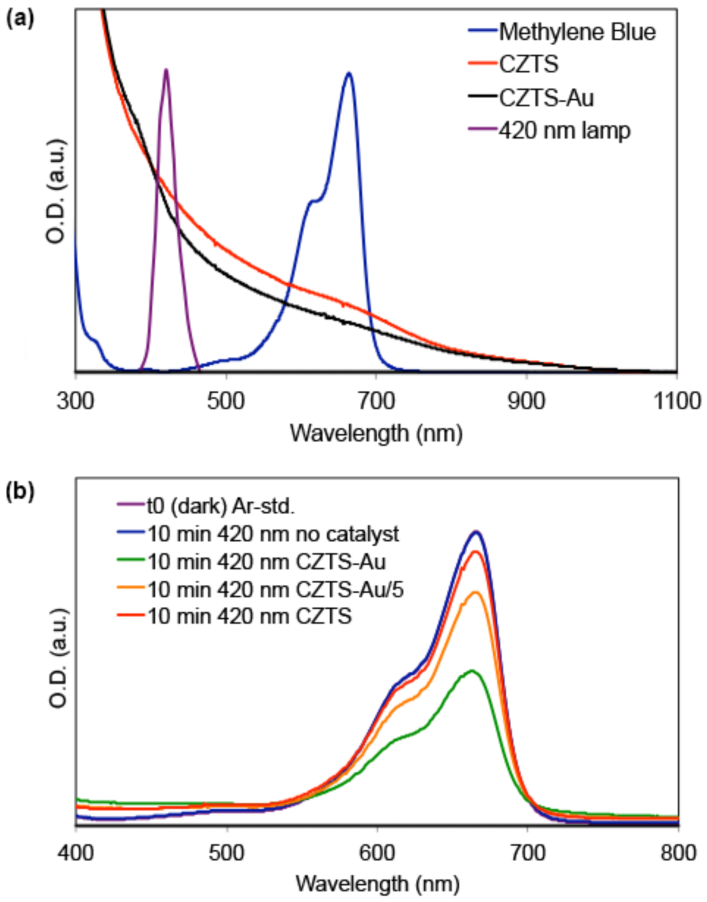

Figure 7. (a) Optical absorption spectra of methylene blue, CZTS and CZTS-Au, and irradiation profile of 420 nm lamps. (b) Optical absorption spectra of methylene blue solutions before and after several representative photocatalytic tests under 420 nm

illumination and in the absence or presence of different concentrations of CZTS-Au and CZTS.

Figure 7b shows optical absorption spectra of methylene blue solutions before and after photocatalytic tests used to probe the reactivity of CZTS-Au. Without a catalyst, the peak at λ_{max} = 663 attributed to methylene blue remains virtually unchanged after 10 min illumination with the 420 nm lamps. However, when CZTS-Au was present the peak intensity decreased by 47% (see Experimental for details). This represents a significant reduction in the amount of methylene blue (Figure 8). When the concentration of CZTS-Au was cut by 1/5, we saw a 17% conversion of methylene blue. Without metal islands on its surface, using CZTS alone only resulted in about 2% conversion. These data are consistent with the fact that noble metal islands on the surface of semiconductor nanocrystals greatly increase photocatalytic activity. Interestingly, the photocatalytic activity of CZTS-Au remained and in some cases even increased after storage in the dark for 60 days (not shown).

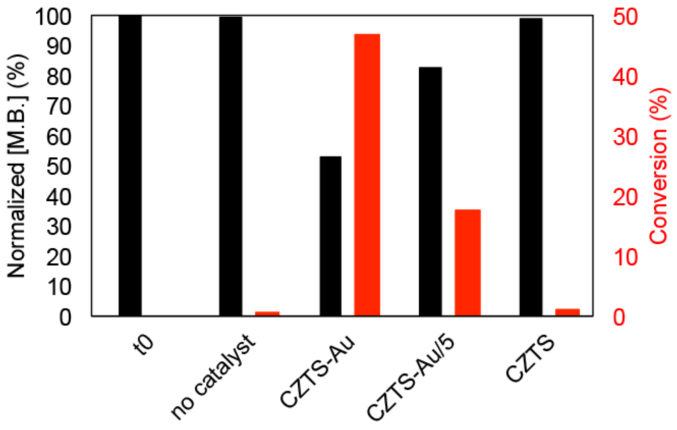

Figure 8. Bar graph showing relative concentrations of methylene blue (M.B.) and its colorless, reduction product leucomethylene blue (L.B.) after 420 nm illumination for 10 min in the absence or presence of different concentrations of CZTS-Au and CZTS.

Metal Removal By Amalgamation. An interesting concept in nanochemistry is the ability not only to build and assemble nano building blocks into more complex edifices but also to break apart and disassemble higher order structures into their separate components.[6] With this in mind, we sought to probe whether Au nanoparticle islands can be removed from the CZTS-Au heterostructures to produce gold-free CZTS nanorods. To this end, we treated CZTS-Au heterostructures with a very small amount of liquid mercury metal (Hg, see Experimental).[65-71] Powder XRD analysis shows that two distinct phases form as a consequence of this treatment, namely: A new solid HgAu amalgam, and wurtzite CZTS. Consecutive, selective centrifugation allows separating these two phases, at least partially (Figure 8). The AuHg amalgam "crashes" or precipitates out of solution first. This AuHg amalgam is comprised of large, 10-20 nm particles characterized by their very dark contrast in bright field TEM due to their high apparent atomic number (Z) compared to CZTS (Figure 8a). Likely due to their high affinity for soft surfaces, the AuHg amalgam particles remain

bound to a few CZTS nanorods. After a couple of centrifugation cycles, wurtzite CZTS becomes the dominant phase observed by XRD and TEM, and the characteristic Au plasmon peak is no longer visible in the optical absorption spectrum (Figures 8b,c). All small Au particles or islands disappear in favor of larger AuHg ones upon amalgamation.

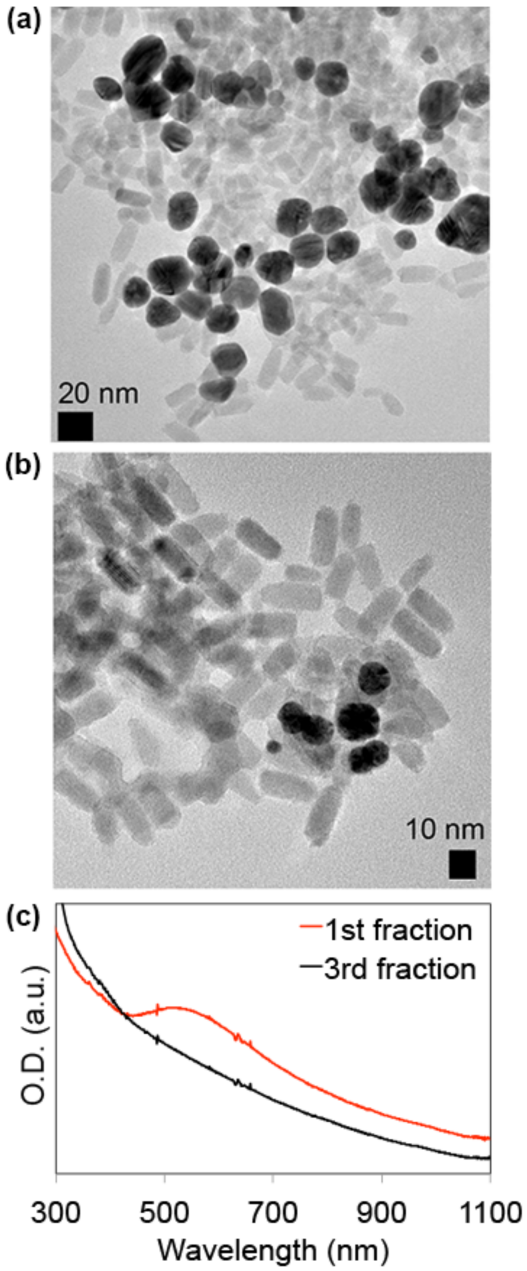

Figure 9. Representative (a, 1st fraction) (b, 3rd fraction) TEM images and (c) optical absorption patterns of different consecutive centrifuged fractions obtained after treatment of CZTS-Au heterostructures with a small amount of Hg.

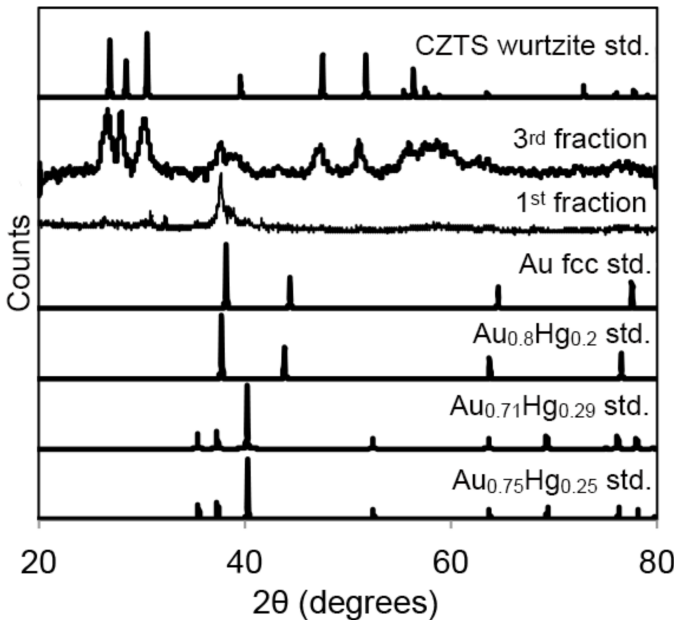

Figure 10. XRD diffraction patterns of different consecutive centrifuged fractions obtained after treatment of CZTS-Au heterostructures with a small amount of Hg. Standard bulk patterns for wurtzite (hexagonal) ZnS (in lieu of CZTS),[48] and metallic (fcc) Au and AuHg alloys are shown for comparison.

Conclusions

We explored the fabrication of CZTS-Au heterostructures by a variety of pathways utilizing both a molecular gold precursor ($AuCl_3$) and preformed Au nanoparticles under thermal and photochemical deposition conditions. The high degree of binding (64-87%) observed when using preformed Au nanoparticles demonstrated the high affinity of nano gold for the soft chalcogenide CZTS surface; however, this binding was incomplete. Using a molecular gold precursor consistently resulted in a higher degree of surface bound Au nanoparticles than using preformed Au nanoparticles. Further, our results show that thermal deposition with a molecular precursor leads to a more controlled reaction with a homogenous distribution of similar-sized Au metal islands along the whole length of CZTS nanorods.

We also demonstrated that CZTS-Au heterostructures are active photocatalysts, able to reduce methylene blue upon irradiation in the presence of a sacrificial electron donor (terminal reductant). Our results indicate that CZTS-Au is a much more active catalyst than CZTS alone, showing the synergy that makes heterostructures capable of undergoing photoinduced charge separation so attractive. We showed that CZTS-Au heterostructures are fairly robust, maintaining photocatalytic activity even after sixty days of dark storage. Treatment of CZTS-Au with a small amount of Hg led to the removal of small Au metal islands on the surface of the CZTS nanorods. The resulting AuHg amalgam remained difficult to separate completely from CZTS, however these results demonstrate a method for breaking down a heterostructure into its individual components. In summary, CZTS-metal heterostructures are accessible by a variety of synthetic pathways, and show promise for potential applications in solar-to-chemical conversion.

Methods

Materials Copper(II) acetylacetonate ($Cu(acac)_2$, 99.99%), methylene blue (>82%), mercury (Hg, 99.99%), dodecylamine (98%), didodecyldimethylammonium bromide (98%), 1-dodecylthiol (98%), tert-dodecylthiol (98.5%), trioctylphosphine oxide (TOPO, 99%) and toluene (anhydrous, 99.8%) were purchased from Sigma-Aldrich. Zinc acetate dihydrate ($Zn(OAc)_2•2H_2O$, 98+%), gold(III) chloride (99.9%) and hydrogen tetrachloroaurate hydrate (chloroauric acid hydrate or $HAuCl_4•H_2O$, 99.9%) were purchased from Strem Chemicals. Tetra-n-octylammonium bromide (98%), sodium borohydride (99%), mercaptosuccinic acid

(99%) and 1-octadecene (ODE, 90%) were purchased from Acros. Tin(IV) acetate ($Sn(OAc)_4$, 98%) and tetramethylammoniumhydroxide pentahydrate (98%) were purchased from Alfa Aesar. Materials were used as received.

Synthesis of Precursor Particles. *Colloidal CZTS Nanorods.* CZTS nanorods were prepared according to a previously reported literature procedure. In a typical synthesis, a mixture of 1-dodecylthiol (0.52 mmol) and tert-dodecylthiol (t-DDT, 3.7 mmol) were injected into a stirring mixture of $Cu(acac)_2$ (0.17 mmol), $Zn(OAc)_2•2H_2O$ (0.25 mmol), $Sn(OAc)_4$ (0.25 mmol), TOPO (1.75 mmol) and 1-octadecene (ODE, 5 mL) in a three-neck round bottom (R.B.) flask under argon (Ar) at 120 °C. The solution was heated to 210 °C and kept at this temperature for 30 minutes. After cooling to room temperature (R.T.), the mixture was twice washed with a 1:1:1 mixture of acetone, ethanol and methanol followed by centrifugation at 4,500 rpm for 10 minutes. The product could be readily redispersed in toluene. *Au Nanoparticles.* Au nanoparticles were prepared according to a previously reported literature procedure.[72] In a typical synthesis, chloroauric acid (96.0 mg, 0.283 mmol) was dissolved in de-ionized water (10 mL) and tetra-n-octylammonium bromide (736 mg, 1.35 mmol) was dissolved in toluene (27 mL). The two solutions were combined and stirred vigorously until the gold (brown material) transferred to the organic layer. 1-dodecylthiol (60.5 mg, 0.299 mmol) was then added to the organic layer. A solution of sodium borohydride (131 mg, 3.45 mmol) in de-ionized water (8 mL) added slowly to the mixture while stirring, and stirring continued for 3 h. The organic phase was separated and concentrated under vacuum to a ~10 mL volume. This was washed three times by precipitating with ethanol (10 mL) followed by centrifugation at 4,500 rpm for 10 min. The product could be readily redispersed in toluene.

Synthesis of CZTS-Au Heterostructures. *CZTS Stock Solution.* CZTS nanorods were dissolved in toluene to give an optical density (O.D.) of 1.2 at 800 nm. A 10 mL volume of this solution was degassed, refilled with dry argon, and stored in the dark for ≥ 12 h in a three-neck R.B. flask. **From $AuCl_3$ Precursor.** Under a dry Ar atmosphere, $AuCl_3$ (12.0 mg, 0.04 mmol), dodecylamine (53.2 mg, 0.29 mmol), and didodecyldimethylammonium bromide (38.0 mg, 0.08 mmol) were dissolved in anhydrous toluene (9 mL) and injected into the CZTS nanorod solution *via* syringe. Deposition was then carried out for 15 min by one of two routes: (1) *Thermally* in the dark, in an oil bath pre-equilibrated at 60 °C, or (2) *photochemically,* under 350 nm illumination at room temperature (R.T., 21-24 °C) in a fan-cooled Rayonet photoreactor (Southern New England Ultraviolet Company, Branford, CT) containing a set of 16 side-on fluorescent lamps and equipped with an air-cooling fan. Nonvolatile products were separated by precipitation with a 1:1:1:1 mixture of acetonitrile, ethanol, methanol and acetone followed by centrifugation. The product could be readily dispersible in toluene. **From Au Nanoparticles.** Au nanoparticles (see above) were dissolved in toluene to give an OD of 0.07 at 520 nm and stored in the dark for ≥ 12 h. The Au nanoparticle solution was injected into the CZTS nanorod solution *via* syringe. The deposition reaction was then carried out for 3 h by one of two routes: (1) *Thermally* in the dark, in an oil bath pre-equilibrated at 60 °C, or (2) *photochemically,* under 350 nm illumination at R.T. in a fan-cooled Rayonet photoreactor containing a set of 16 side-on fluorescent lamps and equipped with an air-cooling fan. Nonvolatile products were separated by precipitation with a 1:1:1:1 mixture of acetonitrile, ethanol, methanol and acetone followed by centrifugation. The product could be readily dispersible in toluene.

Transfer of CZTS-Au to Water. CZTS-Au was dissolved in toluene (5 mL) inside a vial. A solution of tetramethylammonium hydroxide pentahydrate (420 mg, 2.32 mmol) and mercaptosuccinic acid (70 mg, 0.466 mmol) in de-ionized water (5.0 mL) was added, and the mixture stirred in the dark overnight. The aqueous layer was separated and washed two times with a 1:1 mixture of acetone and methanol followed by centrifugation at 4,500 rpm for 10 min. The product was readily dispersible in water.

Photocatalytic Reduction of Methylene Blue. Reduction of methylene blue was carried out inside an oven dried quartz cuvette topped with a septum and cap. A typical reaction involved 2.5 mL of 2.4×10^{-5} M of methylene blue in a 1:6 $^{v}/_{v}$ alcohol (methanol or ethanol) to de-ionized water solution. CZTS-Au (0.5 mL of an aqueous solution with an OD of 0.718 at 800 nm) was added to the mixture, degassed by sparging with dry Ar for 15 min, and placed under 420 nm illumination at R.T. in a fan-cooled Rayonet photoreactor containing a set of 16 side-on fluorescent lamps and equipped with an air-cooling fan.

Au-Stripping. 12 mL of CZTS-Au solution with an OD of 0.44 at 800 nm was placed in a glass vial. Mercury (Hg, 103 mg) was added, and the mixture stirred for 12 h in an oil bath pre-equilibrated at 60 °C. The non-mercury organic liquid fraction was collected with a pipette, and the nonvolatile products were separated by precipitation with a 1:1:1:1 mixture of acetonitrile, ethanol, methanol and acetone followed by centrifugation.

Characterization. *Optical absorption spectroscopy* was measured with an Agilent 8453 UV-Vis photodiode array spectrophotometer. *Powder X-ray diffraction* (XRD) was measured using Cu Kα radiation on a Rigaku Ultima U4 diffractometer. *Transmission Electron Microscopy* (TEM) was conducted on carbon-coated copper grids using FEI Tecnai G2 F20 field emission scanning transmission electron microscope (STEM) at 200 kV (point-to-point

resolution <0.25 nm, line-to-line resolution <0.10 nm). *Elemental composition* was characterized by energy-dispersive spectroscopy (EDS). *Particle dimensions* were measured manually or with ImageJ for >200 particles. Average sizes (diameters) are reported ± standard deviations. *X-ray photoelectron spectroscopy* (XPS) was collected on a Physical Electronics 5500 Multitechnique system using a standard Al Kα source. Analysis spot size was 1x1 mm and the sample was mounted on 2-sided tape (3M). The binding energy values were determined using C 1s at 284.8 eV as a reference.

AUTHOR INFORMATION

Corresponding Author

*vela@iastate.edu

ACKNOWLEDGMENT

J.V. gratefully acknowledges the National Science Foundation for funding of this work through the Division of Materials Research, Solid State and Materials Chemistry program (NSF-DMR-1309510). The authors thank Jim Anderegg for assistance with XPS. P.S.D. thanks Jenna Malmquist for assistance with graphics.

References

[1] Kamat, P. V. Meeting the Clean Energy Demand: Nanostructure Architectures for Solar Energy Conversion. *J. Phys. Chem. C* **2007**, *111*, 2834–2860.

[2] Banin, U.; Ben-Shahar, Y.; Vinokurov, K. Hybrid Semiconductor-Metal Nanoparticles: From Architecture to Function. *Chem. Mater.* **2014**, *26*, 97–110.

[3] Vela, J. Molecular Chemistry to the Fore: New Insights into the Fascinating World of Photoactive Colloidal Semiconductor Nanocrystals. *J. Phys. Chem. Lett.* **2013**, *4*, 653–668.

[4] Maeda, K.; Domen, K. Photocatalytic Water Splitting: Recent Progress and Future Challenges. *J. Phys. Chem. Lett.* **2010**, *1*, 2655–2611.

[5] Maeda, K. Photocatalytic Water Splitting Using Semiconductor Particles: History and Recent Developments. *J. Photochem. Photobiol. C* **2011**, *12*, 237–268.

[6] Buck, M.; Schaak, R. Emerging Strategies for the Total Synthesis of Inorganic Nanostructures. *Angew. Chem. Int. Ed.* **2013**, *52*, 6154–6178.

[7] Carbone, L.; Cozzoli, P. Colloidal heterostructured nanocrystals: Synthesis and growth mechanisms. *Nano Today*. **2010**, *5*, 449–493.

[8] Costi, R.; Saunders, A. Banin, U. Colloidal Hybrid Nanostructures: A New Type of Functional Materials. *Angew. Chem. Int. Ed.* **2010**, *49,* 4878–4897.

[9] Vaneski, A.; Susha, A.; Rodriquez-Fernández, J.; Berr, M.; Jäckel, F.; Feldmann, J.; Rogach, A. Hybrid Colloidal Heterostructures of Anisotropic Semiconductor Nanocrystals Decorated with Noble Metals: Synthesis and Function. *Adv. Funct. Mater.* **2011**, *21*, 1547–1556.

[10] Alvarado, S. R.; Guo, Y.; Ruberu, T. P. A.; Tavasoli, E.; Vela, J. Inorganic Chemistry Solutions to Semiconductor Nanocrystal Problems. *Coord. Chem. Rev.* **2014**, *263–264*, 182–196.

[11] Feng, X.; Hu, G.; Hu, J. Solution-phase Synthesis of Metal and/or Semiconductor Homojunction/heterojunction Nanomaterials. *Nanoscale*. **2011**, *3*, 2099–2117.

[12] Cozzoli, P.D.; Pellegrino, T.; Manna, L. Synthesis, Properties and Perspectives of Hybrid Nanocrystals Structures. *Chem. Soc. Rev.* **2006**, *35*, 1195–1208.

[13] Zhang, N.; Liu, S.; Xu, Y-J. Recent Progress on Metal Core@semiconductor Shell Nanocomposites as a Promising Type of Photocatalyst. *Nanoscale*. **2012**, *4*, 2227–2238.

[14] Casavola, M.; Buonsanti, R.; Caputo, G.; Cozzoli, P. Colloidal Strategies for Preparing Oxide-Based Hybrid Nanocrystals. *Eur. J. Inorg. Chem.* **2008**, 837–854.

[15] Liu, S.; Bai, S-Q.; Zheng, Y.; Shah, K.W.; Han, M-Y. Composite Metal-Oxide Nanocatalysts. *ChemCatChem*. **2012**, *4*, 1462–1484.

[16] Kochuveedu, S.; Jang, Y.; Kim, D. A Study on the Mechanism for the Interaction of Light with Noble Metal-metal Oxide Semiconductor Nanostructures for Various Photophysical Applications. *Chem. Soc. Rev.* **2013**, *42*, 8467–8493.

[17] Ni, M.; Leung, K.H.; Leung, D.; Sumathy, K. A Review and Recent Developments in Photocatalytic Water-splitting Using TiO_2 for Hydrogen Production. *Renew. Sust. Energ. Rev.* **2007**, *11*, 401–425.

[18] Alemseghed, M.; Ruberu, T.P.; Vela, J. Controlled Fabrication of Colloidal Semiconductor-Metal Hybrid Heterostructures: Site Selective Metal Photo Deposition. *Chem. Mater.* **2011**, *23*, 3571–3579.

[19] Schlicke, H.; Ghosh, D.; Fong, L.K.; Xin, H.L.; Zheng, H.; Alivisatos, A.P. Selective Placement of Faceted Metal Tips on Semiconductor Nanorods. *Angew, Chem, Int, Ed.* **2013**, *52*, 980–982.

[20] Kraus-Ophir, S.; Ben-Shahar, Y.; Banin, U.; Mandler, D. Perpendicular Orientation of Anisotropic Au-Tipped CdS Nanorods at the Air/Water Interface. *Adv. Mater. Interfaces* **2014**, *1*, 1300030.

[21] Talapin, D. V.; Yu, H.; Shevchenko, E. V.; Lobo, A.; Murray, C. B. Synthesis of Colloidal PbSe/PbS Core-Shell Nanowires and PbS/Au Nanowire-Nanocrystal Heterostructures. *J. Phys. Chem. C* **2007**, *38*, 14049–14054.

[22] Yang, J.; Elim, H. I.; Zhang, Q.; Lee, J. Y.; Ji, W. Rational Synthesis, Self-Assembly, and Optical Properties of PbS-Au Heterogeneous Nanostructures via Preferential Deposition. *J. Am. Chem. Soc.* **2006**, *128*, 11921–11926.

[23] Hu, W.; Liu, H.; Ye, F.; Ding, Y.; Yang, J. A Facile Solution Route for the Synthesis of PbSe-Au Nanocomposites with Different Morphologies. *Cryst. Eng. Comm.* **2012**, *14*, 7049–7054.

[24] Zhang, Y.; Wang, X.; Song, S.; Liu, D.; Wang, C. Synthesis of Monodispersed Au-PbS Hybrid Nanocrystals via a Solid-Liquid Interfacial Reaction. *Cryst. Eng. Comm.* **2012**, *14*, 7552–7555.

[25] Fang, Z.; Wang, X.; Wang, Q.; Wang, C.; Fan, F.; Liu, X. One-Pot Protocol for the Synthesis of PbS-Au Heterodimers Consisting of Au Nanoparticle on PbS Nanooctahedrons. *Micro & Nano Lett.* **2012**, *7*, 101–104.

[26] Ruberu, T. P. A.; Nelson, N. C.; Slowing, I. I.; Vela, J. Selective Alcohol Dehydrogenation and Hydrogenolysis with Semiconductor-Metal Photocatalysts: Toward Solar-to-Chemical Energy Conversion of Biomass-Relevant Substrates. *J. Phys. Chem. Lett.* **2012**, *3*, 2798–2802.

[27] Ha, J. W.; Ruberu, T. P. A.; Han, R.; Dong, B.; Vela, J.; Fang, N. Super-resolution Mapping of Photo-generated Electron and Hole Separation in Single Metal-Semiconductor Nanocatalysts. *J. Am. Chem. Soc.* **2014**, *136*, 1398–1408.

[28] Wu, K.; Rodríguez-Córdoba, W. E.; Yang, Y.; Lian, T. Plasmon-Induced Hot Electron Transfer from the Au Tip to CdS Rod in CdS-Au Nanoheterostructures. *Nano Lett.* **2013**, *13*, 5255–5263.

[29] Linic, S.; Christopher, P.; Ingram, D. Plasmonic Nanostructures for Efficient Conversion of Solar to Chemical Energy. *Nat. Mater.* **2011**, *10*, 911–921.

[30] Wadia, C.; Alivisatos, A. P.; Kammen, D. M. Materials Availability Expands the Opportunity for Large-Scale Photovoltaics Deployment. *Environ. Sci. Technol.* **2009**, *43*, 2072–2077.

[31] Du, P.; Eisenberg, R. Catalysts Made of Earth-abundant Elements (Co, Ni, Fe) for Water Splitting: Recent Progress and Future Challenges. *Energy Environ. Sci.* **2012**, *5*, 6012–6021.

[32] Singh, A.; Spiccia, L. Water Oxidation Catalysts Based on Abundant 1st Row Transition Metals. *Coord. Chem. Rev.* **2013**, *257*, 2607–2622.

[33] Gust, D.; Moore, T.; Moore, A. Solar Fuels *via* Artificial Photosynthesis. *Acc. Chem. Res.* **2009**, *42*, 1890–1898.

[34] Kudo, A.; Miseki, Y. Heterogeneous Photocatalyst Materials for Water Splitting. *Chem. Soc. Rev.* **2009**, *38*, 253–278.

[35] Wang, M.; Chen, L.; Sun, L. Recent Progress in Electrochemical Hydroden Production with Earth-abundant Metal Complexes as Catalysts. *Energy Environ. Sci.* **2012**, *5*, 6763–6778.

[36] Ramasamy, K.; Malik, M. A.; O'Brien, P. Routes to Copper Zinc Tin Sulfide Cu_2ZnSnS_4 a Potential Material for Solar Cells. *Chem. Commun.* **2012**, *48*, 5703–5714.

[37] Zhou, H.; Hsu, W.C.; Duan, H.S.; Bob, B.; Yang, W.; Song, T.B.; Hsu, C.J.; Yang, Y. CZTS Nanocrystals: a Promising Approach for Next Generation Thin Film Photovoltaics. *Energy Environ. Sci.* **2013**, *6*, 2822–2838.

[38] Fan, F.J.; Wu, L.; Yu, S.H. Energetic I-III-VI_2 and I_2-II-IV-VI_4 Nanocrystals: Synthesis, Photovoltaic and Thermoelectric Applications. *Energy Environ. Sci.* **2013**, *7*, 190–208.

[39] Ramasamy, K.; Malik, M.A.; Revaprasadu, N.; O'Brien, P. Routes to Nanostructured Inorganic Materials with Potential for Solar Energy Applications. *Chem. Mater.* **2013**, *25,* 3551–3569.

[40] Shen, S.; Wang, Q. Rational Tuning the Optical Properties of Metal Sulfide Nanocrystals and Their Applications. *Chem. Mater.* **2012**, *25,* 1166–1178.

[41] Zhang, G.; Finefrock, S.; Liang, D.; Yadav, G.; Yang, H.; Fang, H.; Wu, Y. Semiconductor Nanostructure-Based Photovoltaic Solar Cells. *Nanoscale* **2011**, *3*, 2430–2443.

[42] Riha, S.C.; Parkinson, B.A.; Prieto, A.L. Solution-Based Synthesis and Characterization of Cu_2ZnSnS_4 Nanocrystals. *J. Am. Chem. Soc.* **2009**, *131*, 12054–12055.

[43] Riha, S.C.; Fredrick, S.J.; Sambur, J.B.; Liu, Y.; Prieto, A.L.; Parkinson, B.A.; Photoelectrochemical Characterization of Nanocrystalline Thin-Film Cu_2ZnSnS_4 Photocathodes. *ACS Appl. Mater. Inter.* **2011**, *3*, 58–66.

[44] Riha, S.C.; Parkinson, B.A.; Prieto, A.L. Compositionally Tunable $Cu_2ZnSn(S_{1-x}Se_x)_4$ Nanocrystals: Probing the Effect of Se-Inclusion in Mixed Chalcogenide Thin Films. *J. Am. Chem. Soc.* **2011**, *133*, 15272–15275.

[45] Zhao, Y.; Qiao, Q.; Zhou, W.H.; Cheng, X.Y.; Kou, D.X.; Zhou, Z.J.; Wu, S.X. Wurtzite Cu_2ZnSnS_4 Nanospindles with Enhanced Optical and Electrical Properties. *Chem. Phys. Lett.* **2014**, *592,* 144–148.

[46] Regulacio, M.D.; Ye, C.; Lim, S.H.; Bosman, M.; Ye, E.; Chen, S.; Xu, Q.H.; Han, M.Y. Colloidal Nanocrystals of Wurtzite-Type Cu_2ZnSnS_4: Facile Noninjection Synthesis and Formation Mechanism. *Chem. Eur. J.* **2012,** *18*, 3127–3131.

[47] Singh, A.; Geaney, H.; Laffir, F.; Ryan, K. Colloidal Synthesis of Wurtzite Cu_2ZnSnS_4 Nanorods and Their Perpendicular Assembly. *J. Am. Chem. Soc.* **2012**, *134,* 2910–2913.

[48] Thompson, M.; Ruberu, T.P.; Blakeney, K.; Torres, K.; Dilsaver, P.; Vela, J. Axial Composition Gradients and Phase Segregation Regulate the Aspect Ratio of Cu_2ZnSnS_4 Nanorods. *J. Phys. Chem. Lett.* **2013**, *4*, 3918–3923.

[49] Zou, Y.; Su, X.; Jiang, J. Phase-controlled Synthesis of Cu_2ZnSnS_4 Nanocrystals: The Role of Reactivity between Zn and S. *J. Am. Chem. Soc.* **2013**, *135,* 18377–18384.

[50] Alvarado, S. R.; Guo, Y.; Ruberu, T. P. A.; Bakac, A.; Vela, J. Photochemical vs. Thermal Synthesis of Cobalt Oxyhydroxide Nanocrystals. *J. Phys. Chem. C* **2012**, *116*, 10382–10389.

[51] Sakamoto, M.; Fujistuka, M.; Majima, T. Light as a Construction Tool of Metal Nanoparticles: Synthesis and Mechanism. *J. Photoch. Photobio. C.* **2009**, *10*, 33–56.

[52] Langille, M.; Personick, M.; Mirkin, C. Plasmon-mediated Syntheses of Metallic Nanostructures. *Angew. Chem. Int. Ed.* **2013**, *52*, 13910–13940.

[53] Zeng, H.; Du, X-W.; Singh, S.; Kulinich, S.; Yang, S.; He, J.; Cai, W. Nanomaterials *via* Laser Ablation/Irradiation in Liquid: A Review. *Adv. Funct. Mater.* **2012**, *22*, 1333–1353.

[54] Cozzoli, P.D.; Comparelli, R.; Fanizza, E.; Curri, M.L.; Agostiano, A.; Laub, D. Photocatalytic Synthesis of Silver Nanoparticles Stabilized by TiO_2 Nanorods: A Semiconductor/Metal Nanocomposite in Homogenous Nonpolar Solution. *J. Am. Chem. Soc.* **2004**, *126*, 3868–3879.

[55] Mori, K.; Araki, T.; Takasaki, T.; Shironita, S.; Yamashita, H. A New Application of Photocatalysts: Synthesis of Nano-sized Metal and Alloy Catalysts by a Photo-assisted Deposition Method. *Photochem. Photobiol. Sci.* **2009**, *8*, 652–656.

[56] Dukovic, G.; Merkle, M.; Nelson, J.; Hughes, S.; Alivisatos, A.P. Photodeposition of Pt on Colloidal CdS and CdSe/CdS Semiconductor Nanostructures. *Adv. Mater.* **2008**, *20*, 4306–4311.

[57] Menagen, G.; Macdonald, J.; Shemesh, Y.; Popov, I.; Banin, U. Au Growth on Semiconductor Nanorods: Photoinduced versus Thermal Growth Mechanisms. *J. Am. Chem. Soc.* **2009,** *131*, 17406–17411.

[58] Carbone, L.; Jakab, A.; Khalavka, Y.; Sönnichsen, C. Light-Controlled One-Sided Growth of Large Plasmonic Gold Domains on Quantum Rods Observed on the Single Particle Level. *Nano Lett.* **2009**, *9*, 3710–3714.

[59] Pacholski, C.; Kornowski, A.; Weller, H. Site-Specific Photodeposition of Silver on ZnO Nanorods. *Angew. Chem. Int. Ed.* **2004**, *43*, 4774–4777.

[60] Costi, R.; Saunders, A.; Elmalem, E.; Salant, A.; Banin, U. Visible Light-Induced Charge Retention and Photocatalysis with Hybrid CdSe-Au Nanodumbbells. *Nano Lett.* **2008**, *8*, 637–641.

[61] Asahi, R.; Morikawa, T.; Ohwaki, T.; Aoki, K.; Taga, Y. Visible-Light Photocatalysis in Nitrogen-Doped Titanium Oxides. *Science* **2001**, *293*, 269–271.

[62] Burda, C.; Lou, Y.; Chen, X.; Samia, A. C. S.; Stout, J.; Gole, J. L. Enhanced Nitrogen Doping in TiO_2 Nanoparticles. *Nano Lett.* **2003**, *3*, 1049–1051.

[63] Sangpour, P.; Hashemi, F.; Moshfegh, A. Z. Photoenhanced Degradation of Methylene Blue on Cosputtered M:TiO_2 (M = Au, Ag, Cu) Nanocomposite Systems: A Comparative Study. *J. Phys. Chem. C* **2010**, *114*, 13955–13961.

[64] Jakob, M.; Levanon, H.; Kamat, P. V. Charge Distribution between UV-Irradiated TiO_2 and Gold Nanoparticles: Determination of Shift in the Fermi Level. *Nano Lett.* **2003**, *3*, 353–358.

[65] Lin, J-H.; Tseng, W-L. Gold Nanoparticles for Specific Extraction and Enrichment of Biomolecules and Environmental Pollutants. *Rev. Anal. Chem.* **2012**, *31*, 153–162.

[66] Miranda, C.; Yañez, J.; Contreras, D.; Garcia, R.; Jardim, W.; Mansilla, H. Photocatalytic Removal of Methylmercury Assisted by UV-A Irradiation. *Appl. Catal. B.* **2009**, *90*, 115–119.

[67] Lisha, K.P.; Pradeep, T. Towards a Practical Solution for Removing Inorganic Mercury from Drinking Water using Gold Nanoparticles. *Gold Bulletin.* **2009**, *42*, 144–152.

[68] Ojea-Jiménez, I.; López, X.; Arbiol, J.; Puntes, V. Citrate-Coated Gold Nanoparticles As Smart Scavengers for Mercury(II) Removal from Polluted Waters. *ACS Nano.* **2012**, *6*, 2253–2260.

[69] Pacheco, S.; Medina, M.; Valencia, F.; Tapia, J. Removal of Inorganic Mercury from Polluted Water Using Structured Nanoparticles. *J. Environ. Eng.* **2006**, 342–349.

[70] Qian, H.; Pretzer, L.; Velazquez, J.; Zhao, Z.; Wong, M. Gold Nanoparticles for Cleaning Contaminated Water. *J. Chem. Technol. Biotechnol.* **2013**. *88*, 735–741.

[71] Gong, Y.; Liu, Y.; Xiong, Z.; Kaback, D.; Zhao, D. Immobilization of Mercury in Field Soil and Sediment using Carboxymethyl Cellulose Stabilized Iron Sulfide Nanoparticles. *Nanotech.* **2012**, *23*, 1–13.

[72] Brust, M.; Walker, M.; Bethell, D.; Schiffrin, D. J.; Whyman, R. Synthesis of Thiol-derivatized Gold Nanoparticles in a 2-phase Liquid-liquid System. *J. Chem. Soc., Chem. Commun.* **1994**, 801–802.

CHAPTER 3

GENERAL CONCLUSIONS

In summary, we were able to prepare CZTS-Au heterostructures with demonstrated photocatalytic properties. CZTS-Au was prepared in 4 separate pathways, utilizing $AuCl_3$ or pre-formed Au NPs under thermal or photochemical conditions. The precursor and conditions greatly affected the quality of the resulting heterostructures. It was determined for our system that using $AuCl_3$ under thermal conditions resulted in the most well-defined, monodisperse product with a high number of small Au NPs per nanorod.

We were further able to demonstrate that Au NPs could be removed after the deposition process. To do this we utilized the affinity that Hg has for Au. Although there was no sign of small Au NPs remaining on the CZTS nanorods, it was apparent that larger Au-Hg amalgams were still bound to the soft surface of CZTS and these larger amalgams were not separable from the CZTS nanorods. This work demonstrates the ability to break apart higher-ordered heterostructures into their components and remains an important goal in the control over nanoscale materials.

After synthesizing these heterostructures and demonstrating control over them, we then chose the model system of methylene blue to demonstrate the photocatalytic properties of CZTS-Au. The heterostructures successfully reduced methylene blue with a conversion rate similar to that reported for CdSe-Au. Furthermore CZTS-Au had a significantly higher conversion rate than CZTS alone which is consistent with the view that metal islands can greatly increase photocatalytic activity. Further studies showed the catalyst remained active after 60 days storage in water demonstrating the robustness of the material. We believe this

may be in part due to the stabilizing effect of Au metal islands on the CZTS nanorods, which is yet another potential benefit to these heterostructures.

This work represents progress toward the goal of finding more earth-abundant, non-toxic materials for use in solar energy conversion. We can achieve similar conversion rates to that of CdSe-Au utilizing a material with more abundant and less toxic elements. The material is also fairly robust and can be stored in water. Future work will center on testing the activity of the material in more useful photocatalytic reactions.